

PRESERVATION OF CUSPY PROFILES IN DISK GALAXY MERGERS

Héctor Aceves¹ & Héctor Velázquez

Instituto de Astronomía, UNAM, Ensenada

Received ——; *accepted* ——

RESUMEN

Se efectuaron tres simulaciones auto-consistentes de N -cuerpos de fusiones binarias entre galaxias espirales. Inicialmente estos encuentros siguen órbitas parabólicas. Los modelos de galaxias progenitoras incluyen tanto un disco estelar como el momento angular intrínseco del halo. La razón de masas de las galaxias progenitoras es alrededor de 1:1, 1:3 and 1:10. Encontramos que el perfil de densidad inicial pronunciado de los halos oscuros es preservado en las fusiones para los casos considerados aquí.

ABSTRACT

We have carried out three self-consistent N -body simulations of binary mergers between spiral galaxies. Initially, these encounters follow parabolic orbits. Progenitor galaxy models include both a stellar disk as well as the halo's intrinsic angular momentum. The mass-ratio for the disk galaxy progenitors is about 1:1, 1:3 and 1:10. We find that the initial cuspy density profile of the dark halos is preserved after merging for the cases considered here.

Key Words: **GALAXIES: KINEMATICS AND DYNAMICS – GALAXIES: DARK MATTER – METHODS: N-BODY SIMULATIONS.**

1. INTRODUCTION

High-resolution simulations of hierarchical structure formation within a Λ CDM cosmogony show that the inner regions of the halos follow a power-law cusp, $\rho \propto r^{-\gamma}$, with $1 \leq \gamma \leq 1.5$ while in their outer parts the profiles go as $\rho \propto r^{-3}$ over a wide range of mass-scales (e.g., Navarro, Frenk & White 1997, hereafter NFW, Moore et al. 1999, hereafter M99, Fukushige, Kawai & Makino 2004, Navarro et al. 2004).

The physical origin of this profile is still unclear and it is the subject of an intense investigation. Nevertheless, there is a certain agreement in the sense that a such density profile is linked to the accretion and merging history of the dark matter substructures (e.g., Syer & White 1998, Dekel, Devor & Hetzroni 2003, Williams, Babul & Dalcanton 2004).

Several studies indicate that angular momentum may play a key role at the time of formation of the halo as well as on the shape of the density profile within the inner regions by preventing that dark matter particles reach the inner regions, ending in

a shallower central profile (e.g., White & Zaritsky 1992, Hiotelis 2002, Ascasibar et al. 2004). In this work we test the role of the spin of the dark halo in shaping the profile of the resulting remnant. Boylan-Kochin & Ma (2004, hereafter BKM) have recently addressed this question. These authors find that if two galaxies merge having each one a core-type profile the resulting remnant will be core-type, and if one progenitor has a cuspy profile then the remnant will also be cuspy. However, BKM do not consider the effect of a luminous component, as a disk, and the spin of the halos. Furthermore, their study was restricted to head-on encounters.

In this work we study three numerical N -body simulations of progenitor self-consistent disk galaxies with mass-ratios of about 1:1, 1:3 and 1:10 and following parabolic encounters. Halos have spin and galaxy disks are built up within a model of disk galaxy formation (Mo, Mao & White 1998). This would allows us to test if the cuspy nature of the progenitor galaxies is preserved at the resolution provided by our N -body simulations.

The rest of this paper has been organized as fol-

¹Email: aceves@astrosen.unam.mx

lows. In §2 we describe the theoretical method used to construct the galaxy models, the properties of their dark halos, especially the behavior of the inner logarithmic derivative, $\beta(r) = d \log \rho / d \log r$, and the initial conditions for the encounters. In §3 we present our results, and in §4 we summarize our main results.

2. MERGER MODEL

2.1. Disk Galaxies

Our galaxy models consist of a spherical halo and a stellar disk; no bulge component is included. The disk is represented by an exponential profile in the radial direction and by an isothermal sheet in the vertical one (Hernquist 1993):

$$\rho_d(R, z) = \frac{M_d}{4\pi R_d^2 z_d} \exp(-R/R_d) \operatorname{sech}^2(z/z_d), \quad (1)$$

where R_d and z_d are the radial and vertical scale-lengths of the disk, respectively.

For the dark halo, a spherical model is adopted by assuming a NFW-profile with an exponential cutoff:

$$\rho_h(r) = \frac{M_h \alpha_h}{4\pi r(r + r_s)^2} \exp\left[-\left(\frac{r}{r_{200}} + q\right)^2\right], \quad (2)$$

where r_s and r_{200} , are the the scale and virial radii, respectively. $c = q^{-1} = r_{200}/r_s$ and M_h are the concentration and the mass of the halo. Here, α_h is a normalization constant given by

$$\alpha_h = \frac{\exp(q^2)}{\sqrt{\pi}q \exp(q^2) \operatorname{Erfc}(q) + \frac{1}{2} \exp(q^2) \operatorname{E}_1(q^2) - 1}$$

being $\operatorname{Erfc}(x)$ the complimentary error function and $\operatorname{E}_1(x)$ the exponential integral.

The radial scale length of the disk is obtained accordingly to the Mo, Mao & White (1998) framework of disk galaxy formation. To determine this quantity five parameters are required, namely: the circular velocity V_c at r_{200} , the dimensionless spin parameter λ , the concentration c of the dark halo, the fraction of disk to halo mass m_d , and the fraction of angular momentum in the disc to that in the halo j_d . We followed the method described by Shen, Mo & Shu (2002) to obtain these parameters. A Λ CDM cosmology is adopted with a mass density of $\Omega_0 = 0.3$ and with a contribution due to the cosmological constant of $\Omega_\Lambda = 0.7$.

The selected galaxy disks satisfy the stability criterion $\varepsilon_m \geq 0.9$; where $\varepsilon_m = V_m (GM_d/R_d)^{-1/2}$, being

V_m the maximum rotation velocity (Efstathiou, Lake & Negroponte 1982, Syer, Mao & Mo 1997). Mass-ratios of about 1:1, 1:3 and 1:10 were chosen to study the properties of the merger remnants. Finally, velocities of particles were set up through Jeans equations following the method prescribed by Hernquist (1993).

In Table 1 we list the parameters defining our galaxy models; below the merger simulation label ($S1$, $S2$, and $S3$) the mass ratio of the secondary to the primary galaxy has been indicated. The number of particles in the halo N_h and in the disk N_d are also listed.

2.2. Encounter Parameters

Only parabolic encounters are considered for the binary mergers. The relative initial separation between both galaxy centers is taken to be

$$R_s = 1.25 (r_{200,1} + r_{200,2}); \quad (3)$$

where $r_{200,1}$ and $r_{200,2}$ are, respectively, their r_{200} virial radii.

Orbital angular momentum is introduced in the simulations by randomly choosing a pericenter for each encounter, assuming that galaxies are point particles in a Keplerian orbit. Pericentric radii in the range $R_p = \{5 - 20\}$ kpc were adopted. These values for the orbital parameters are consistent with those found in cosmological N -body simulations and tend to favor mergers (Navarro, Frenk & White 1995). The relative orientation of the spin vector of the galaxies, relative to the orbital plane of the encounter, is chosen randomly.

2.3. Numerical Tools

These N -body simulations were performed using a parallel version of GADGET, a tree base code with individual timesteps (Springel, Yoshida & White 2001). The runs were made in a Pentium based cluster of 32 processors (Velázquez & Aguilar 2002). Softening parameters $\epsilon_d = 35$ pc and $\epsilon_h = 350$ pc for disk and halo particles, respectively, were used. Since GADGET uses a spline kernel for the softening, the gravitational interaction between two particles is fully Newtonian for separations larger than twice the softening parameters (Power et al. 2003).

The typical time of arrival of the galaxies to the first passage through pericenter is about 1 Gyr. We follow each encounter for a total time of about 8 Gyr. At this time the remnants had reached virial equilibrium. Energy conservation was better than 0.25% in all these simulations.

TABLE 1
INITIAL GALAXIES

Merger M_s/M_p	Halo Properties						Disc Properties			
	M_h [M_\odot]	r_{200} [kpc]	λ	j	c	N_h	M_d [M_\odot]	R_d [kpc]	z_d [kpc]	N_d
$S1$ 0.14	4.74×10^{11} 6.99×10^{10}	110.3 58.3	0.112 0.071	0.106 0.035	11.39 9.94	240000 165992	4.16×10^{10} 2.88×10^9	6.6 1.6	1.29 0.19	60000 48689
$S2$ 0.32	4.02×10^{11} 1.25×10^{12}	104.3 152.3	0.063 0.056	0.041 0.068	7.63 3.84	57126 177571	2.11×10^{10} 7.78×10^{10}	2.4 5.7	0.39 0.47	12000 44267
$S3$ 0.98	8.11×10^{10} 8.33×10^{10}	61.2 61.8	0.099 0.122	0.142 0.095	10.87 10.01	150000 154050	7.22×10^9 7.15×10^9	4.6 3.9	0.73 0.56	30000 29686

TABLE 2
INITIAL GALAXY SLOPES

Merger M_s/M_p	N-body Model		
	RMS	RMS ₁₀	$-\beta_c$
$S1$	0.098	0.046	1.25
	0.115	0.068	1.22
$S2$	0.128	0.105	1.28
	0.178	0.120	1.06
$S3$	0.102	0.075	1.12
	0.100	0.053	1.32

2.4. Resolution Criteria

The two-body relaxation time-scale imposes an inner ‘convergence’ radius r_c over which the stellar system can be adequately described by a collisionless distribution function (e.g., Power et al. 2003; Hayashi et al. 2004; Diemand et al. 2004; Binney 2004).

Here, we take r_c as the radius where its local two-body relaxation time-scale t_r is longer than the period T_v of a circular orbit at the virial radius,

$$\frac{t_r(r)}{T_v} = \frac{N}{8 \ln N} \frac{r}{V} \frac{V_v}{r_v}, \quad (4)$$

where V_v the circular velocity at the virial radius, r_v , and $N=N(r)$ the total number of particles inside a radius r . The virial radius is $r_v=GM_t/|W|$, being M_t the total mass of all bound particles and W its total potential energy.

We computed spherically averaged density profiles, $\rho(r)$, for each initial galaxy in a logarithmically spaced grid within r_c and r_v ; in general, we find $r_c/r_v \approx 0.01$. To check that the dark density profile of our initial galaxy models does not change, we evolved in isolation each galaxy for about 5 Gyrs. No significant change in the density profiles was observed.

We fitted NFW density profiles,

$$\rho_*(r) = \frac{\rho_s}{(r/\bar{r}_s)(1+r/\bar{r}_s)^2}, \quad (5)$$

to the $\rho(r)$ of the initial numerical models; where \bar{r}_s is the scale radius. The fitting was done by χ^2 -minimization using the Levenberg-Marquart method (Press et al. 1992). From the fitted profile we computed the logarithmic derivative $\beta(r)$.

To verify that our binning method does not affect the fitting of the density profiles, we computed $\rho(r)$ in bins of equal number of particles, from 100 to 1500, and the parameters of the fitted profile did not changed significantly ($\lesssim 1\%$) in comparison to the logarithmically spaced grid. We consider this provides a good degree of confidence on the results presented for our fits.

The mean RMS of the deviations, $\delta = (\rho - \rho_*)/\rho$, for the initial profiles in the complete fitting interval is 0.120, while for the inner region up to a radius of 10% the virial radius a mean, RMS₁₀, of 0.078 is obtained. The latter value for the RMS provides an indication of how good the quality the N -body realization follows the initial profile at the inner regions.

We estimated the logarithmic derivative at r_c , β_c , for each individual galaxy, and a mean value of -1.21 is found. Individual values of β_c and RMS, both total and inside $0.10R_v$, are listed in Table 2.

3. MERGER DENSITY PROFILES

In Figure 1 we show snapshots of the evolution of simulation $S2$ in Table 1. The elapsed time, in Gyr, is indicated in each snapshot. Common features found in earlier studies of merging galaxies (e.g., Barnes 1998), such as tidal distortions, are observed for the dark halos.

A NFW profile was fitted to the resulting merger remnant. The fitting is done in their corresponding interval r_c to r_v . In Table 3 we present the values

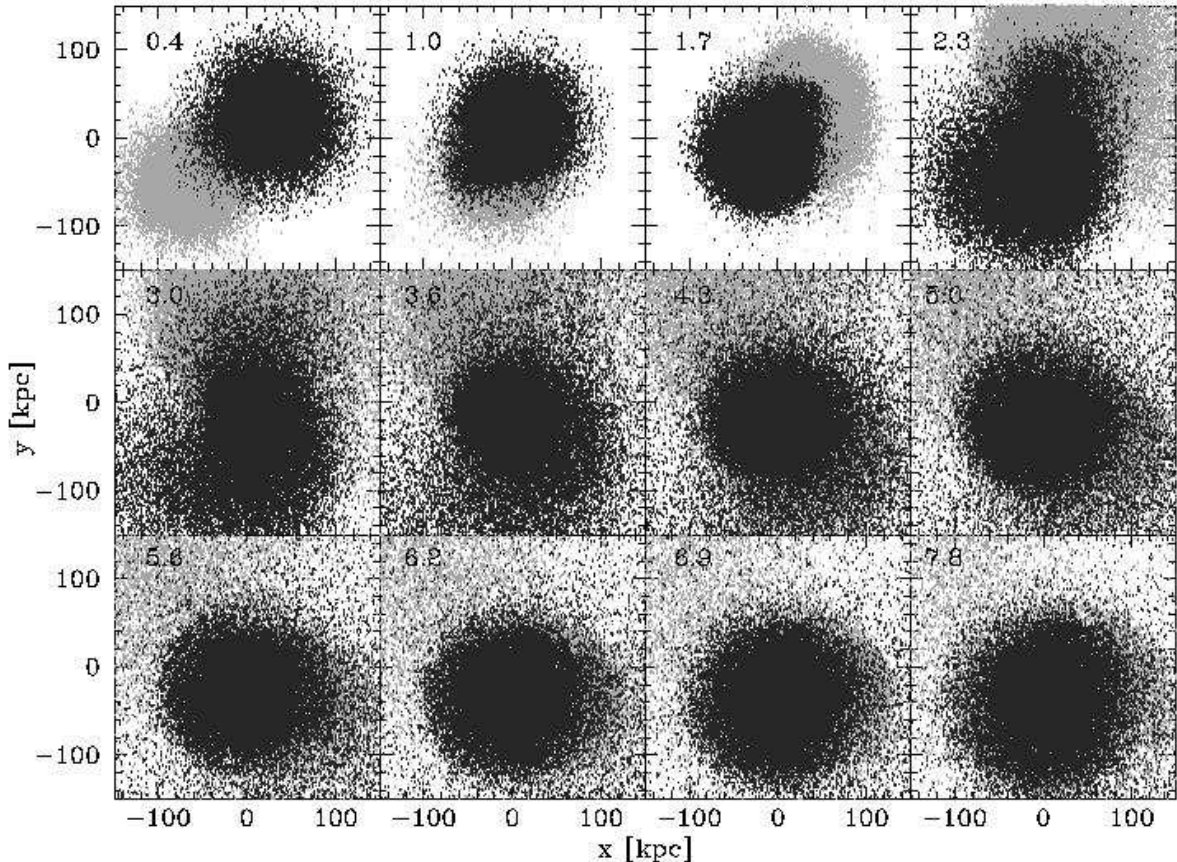


Fig. 1. Snapshots of the evolution the dark halos of simulation $S2$. Numbers indicate time in Gyr. Lighter color indicates the secondary galaxy of this merger. Boxes are 300 kpc on each side. The first pericenter passage is reached at ≈ 1 Gyr.

TABLE 3
REMNANTS' NFW PROFILE.

Merger	Profile Parameters				
	RMS	RMS ₁₀	\bar{r}_s	\bar{c}	$-\beta_c$
$S1$	0.074	0.040	5.69	13.17	1.24
$S2$	0.124	0.078	24.40	6.39	1.12
$S3$	0.082	0.081	4.42	14.96	1.37

for the total RMS deviation of the data to the fitted NFW profile (column 2), the RMS inside 10% of the virial radius (column 3), the scale radius \bar{r}_s in kpc (column 4), the concentration parameter $\bar{c} = r_v/\bar{r}_s$ (column 5), and the logarithmic derivative at r_c obtained from the fitting (column 6).

In Figure 2 (*top*) we show the fractional residuals of the merger fittings and (*bottom*) the numerical logarithmic derivatives of the data that correspond to the fitted profile (5). Though the numerical logarithmic derivatives are rather noisy, especially at the boundaries of the fitting region, they follow in av-

erage the $\beta(r)$ obtained from the fits. The average RMS of the density fits for the entire interval is 0.093, while for the region up to $0.10r_v$ is about 0.066. On the other hand, the average value of β_c obtained for the remnants is -1.24 .

The mean RMS₁₀ of mergers is close by less than 15% to the one found for the fits of a NFW profile to the initial galaxies. The same behavior is found for the $\langle\beta_c\rangle$. This indicates that the initial degree of cuspyness of the progenitors is preserved after the merging process for the cases treated here.

There has been some discussion (e.g., Navarro et al. 2004) if a profile of the form proposed by M99,

$$\rho(r) = \frac{\rho_M}{(r/r_M)^{1.5}[1 + (r/r_M)^{1.5}]} , \quad (6)$$

provides a better fit to dark halos. We tested also if (6) provided a better fit to the density profiles of the remnants. In Table 4 we list the values obtained for similar quantities as shown in Table 3; but with $\tilde{c} = r_v/r_M$. In Figure 3 we show the fractional residuals of the fits and $\beta(r)$ using (6).

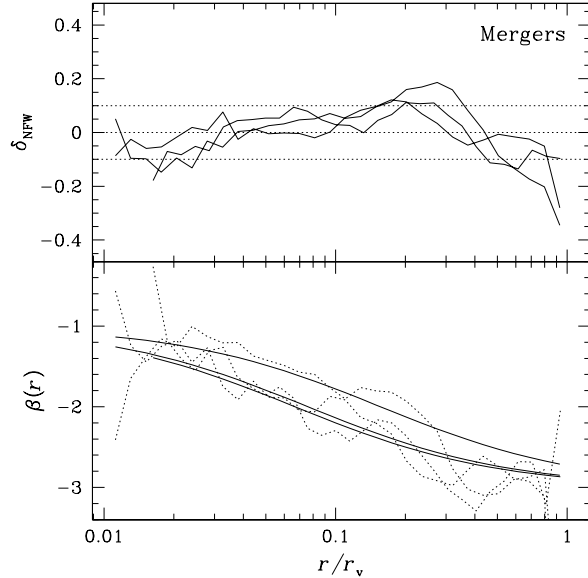


Fig. 2. (Top) Fractional residuals, $\delta_{\text{NFW}} = (\rho - \rho_{\text{NFW}})/\rho$, of the initial N -body galaxy density profiles with respect a NFW profile. (Bottom) Numerical logarithmic derivatives (dotted lines) and the ones obtained from the fitted profile (continuous lines).

TABLE 4
REMNANTS' M99 PROFILE.

Merger	Profile Parameters				
	RMS	RMS ₁₀	r_M	\tilde{c}	$-\beta_c$
S1	0.084	0.093	10.56	7.09	1.53
S2	0.196	0.219	47.03	3.32	1.51
S3	0.077	0.099	7.98	8.29	1.56

We find a mean $\beta_c = -1.53$ but with the average RMS₁₀ to be 0.137. A value that is $\approx 100\%$ larger than that obtained with the NFW profile inside $0.1R_v$. We take this result as an indication that the M99 profile does not provide a good fit to our merger remnants' profiles.

4. SUMMARY

We have constructed disk galaxies using the cosmologically motivated model of MMW to study the cuspyness properties of the merger remnants. These progenitor galaxies have spin in their halos and mass-ratios of about 1:10, 1:3, and 1:1. This work was restricted to study binary mergers following parabolic encounters.

Our results indicate that angular momentum, both intrinsic and orbital, do not change the behavior of the density profile inside the inner regions of a merger remnant. In particular, the initial profile

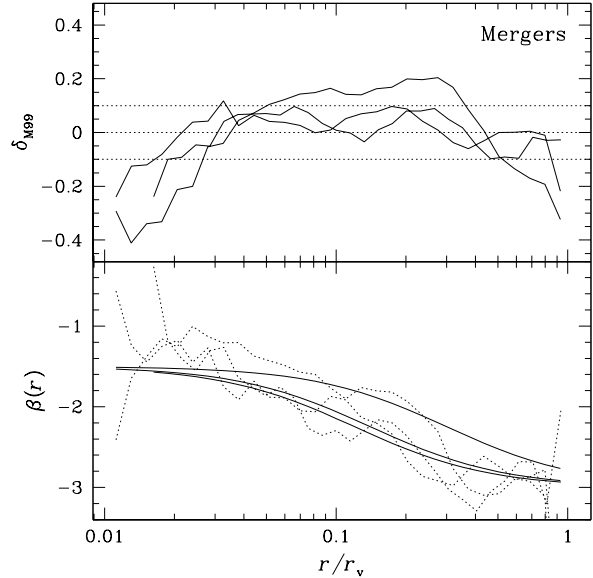


Fig. 3. (Top) Fractional residuals, $\delta_{\text{M99}} = (\rho - \rho_{\text{M99}})/\rho$, of the initial N -body galaxy density profiles with respect a M99 profile. (Bottom) numerical logarithmic derivatives (dotted lines) and the ones obtained from the assumed profile (continuous lines).

of progenitors appear rather robust against a mass-spectrum and angular momentum.

However, taking into account that these are rather that a few simulations, we can not completely rule out the effect of the initial angular momentum on the inner density profile of the remnants. A more wider set of simulations is required to test the result found here. This work is underway.

Acknowledgments

We thank CONACyT, México, for financial support through Project 37506-E.

REFERENCES

- Ascasibar Y., Yepes G., Gottlöber, Müller V., 2004, MNRAS, 352, 1109
- Barnes J., 1998, in Friedli D., Martinet L. and Pfenniger D., eds, Galaxies: Interactions and Induced Star Formation, Saas-Fee Advance Course 26, Springer-Verlag, N. Y.
- Binney J., 2004, MNRAS, 350, 939
- Boylan-Kolchin M., Ma C., 2004, MNRAS, 349, 1117 (BKM)
- Dekel A., Devor J., Hetzroni G., 2003, 341, 326
- Diemand J., Moore B., Stadel J., Kazantzidis S., 2004, MNRAS, 348, 977
- Efstathiou G., Lake G., Negroponte J., 1982, MNRAS, 199, 1069
- Fukushige T., Kawai A., Makino J., 2004, ApJ, 606, 625

Hayashi E., Navarro J. F., Power C., Jenkins A., Frenk C. S., White S. D. M., Springel V., Stadel J., Quinn T. R., 2004, MNRAS, 355, 794

Hernquist L., 1993, ApJS, 86, 389

Hiotelis N., 2002, A&A, 382, 84

Mo H. J., Mao S., White S. D. M., 1998, MNRAS, 295, 319 (MMW)

Moore B., Quinn T., Governato F., Stadel J., Lake G., 1999, MNRAS, 310, 1147 (M99)

Navarro J. F., Frenk C. S., White S. D. M., 1995, MNRAS, 275, 56

Navarro J. F., Frenk C. S., White S. D. M., 1997, ApJ, 490, 493 (NFW)

Navarro J. F., Hayashi E., Power C., Jenkins A. R., Frenk C. S., White S. D. M., Springel V., Stadel J., Quinn T. R., 2004, MNRAS, 349, 1051

Press W. H., Teukolsy S. A., Vetterling W. T., Flannery B. P., 1992, Numerical Recipes: The Art of Scientific Computing. Cambridge Univ. Press, New York

Power C., Navarro J. F., Jenkins A., Frenk C. S., White S. D. M., Springel V., Stadel J., Quinn T., 2003, MNRAS, 338, 14

Shen S., Mo H. J., Shu C., 2002, MNRAS, 331, 251

Springel V., Yoshida N., White S. D. M., 2001, New Astronomy, 6, 79

Syer D., White S. D. M., 1998, MNRAS, 293, 337

Syer D., Mao S., Mo H. J., 1997, [astro-ph/9711160](#)

Velázquez H., Aguilar L. 2003, RMxAA, 39, 197

White S. D. M., Zaritsky D., 1992, ApJ, 394, 1

Williams L. L. R., Babul A., Dalcanton J. J., 2004, ApJ, 604, 18